Theoretical Computer Science 607 (2015) 363–380

Contents lists available at ScienceDirect

Theoretical Computer Science

www.elsevier.com/locate/tcs

A better approximation for constructing virtual backbone in 3D wireless ad-hoc networks

Xiaofeng Gao *, Jun Li, Guihai Chen

Shanghai Key Laboratory of Scalable Computing and Systems, Department of Computer Science and Engineering, Shanghai Jiao Tong University, 200240, Shanghai, PR China

ARTICLE INFO

Article history:
Received 31 March 2015
Received in revised form 22 July 2015
Accepted 31 July 2015
Available online 7 August 2015

Keywords:
Wireless ad-hoc network
Virtual backbone
Connected dominating set (CDS)
Unit ball graph

ABSTRACT

Wireless ad hoc networks have been widely used in many areas. In order to improve network performance, we often select a connected dominating set (CDS) as its virtual backbone to deal with routing-related tasks. The problem of finding a minimum CDS (MCDS) for 2-dimensional networks has been widely studied, whereas finding an MCDS in 3-dimensional networks draws more attention recently, because it can formulate the network environment more precisely. Since MCDS problem is proved to be NP-complete, lots of approximations were proposed in literature. Among those, the best approximation for MCDS in 3D network is 14.937 in [1]. However, their projection method during the approximation deduction process is incorrect, which overthrows its final bound completely. As a consequence, in this paper we will first propose a new projection method to overcome their problem, illustrate the cardinality upper bound of independent points in a graph (which will be used to analyze the approximation ratio), and then optimize the algorithms to select MCDS with prune techniques. The major technique we use is an adaptive jitter scheme, which solves the open question in this area.

1. Introduction

Wireless ad hoc networks consist of lots of wireless nodes, which serve not only as mobile hosts but also as routers. Because of such characteristics, wireless ad hoc networks can be widely used in lots of applications such as sensor monitoring, traffic control, mobile computing, etc. [2–5]. However, those networks do not have physical infrastructures. When any two nodes in a wireless ad hoc network want to communicate with each other, they must forward messages to intermediate nodes to construct route between them. Consequently, this will cause unnecessary energy consumption and even broadcast storm when routing.

To overcome such shortcomings, we usually construct a virtual backbone to response for routing related tasks. A virtual backbone consists of a subset of all nodes in a wireless ad hoc network. Every node in the wireless ad hoc network is either in this subset or adjacent to at least one node of the subset. With virtual backbone, each ordinary node only need to send messages to its surrounding nodes which are in virtual backbone. And the nodes in virtual backbone will help it to forward such messages to its destination. As a result, virtual backbone can greatly reduce forwarding processes in wireless ad hoc networks. In literature, virtual backbone has been widely studied [6–9].

* Corresponding author.
E-mail addresses: gao-xf@cs.sjtu.edu.cn (X. Gao), lijun2009@sjtu.edu.cn (J. Li), gchen@cs.sjtu.edu.cn (G. Chen).

http://dx.doi.org/10.1016/j.tcs.2015.07.061
0304-3975/

For any given wireless ad hoc network, we can represent it by an undirected graph $G = (V, E)$ as follows: any vertex $v \in V$ corresponds to a node in the original network, while any edge $(u, v) \in E$ represents that the nodes corresponding to vertices u and v can communicate with each other. Moreover, it is widely accepted that a connected dominating set (CDS) of the given graph is often the first choice to construct a virtual backbone for the corresponding wireless ad hoc network [10,11]. A CDS is defined to be a subset of V in a given graph $G = (V, E)$, such that every vertex of V is either in this subset or adjacent to a vertex in this subset and this subset can induce a connected subgraph.

Most literature discussed CDS in two-dimensional space, and use a unit disk graph (UDG) to model the network. However, such model cannot precisely describe the non-flat area such as mountainous region [12] or underwater environment [13]. Correspondingly, we can use a unit ball graph (UBG) to model such a network in 3-dimensional space. In a UBG $G = (V, E)$, any two vertices are adjacent (or connected) if and only if the Euclidean distance between them is at most 1.

Since UBG can formulate a network environment more precisely than UDG, CDS in UBG can represent more applications than that in UDG. For instance, Wang et al. [14] constructed 3D landmark maps with vision data extracted from camera images, and then used 3D-CDS to improve data association in application of simultaneous localization and mapping (SLAM). Yang [15] implemented 3D-CDS as clusters to find an optimal topology control strategy in 3D wireless sensor networks. In all, it is significant to design fast algorithms for selecting an appropriate CDS set from a given network and analyze their performance. Typically, a CDS with minimum cardinality is the most efficient choice for practical use, and we refer it as MCDS.

Finding a minimum CDS (MCDS) is a well-known NP-complete problem, and lots of approximation algorithms were proposed during last decade. Those algorithms often include two phases. Firstly, they choose a maximal independent set (MIS) from G. Second, they add some extra nodes from G to connect this MIS, usually by Steiner trees. An MIS in a graph $G = (V, E)$ is a subset $M \subseteq V$ such that any two vertices from M are not connected and we cannot add another vertex from $M \backslash V$ to form a bigger MIS. Easy to see, in UDG or UBG, the distance between any two vertices in M should be more than 1.

In 2-dimensional situation, the approximation ratio of such algorithms has been widely studied. Based on the fact that the neighborhood area of any node can contain at most five independent points, Wan et al. [16] proposed that $mis(G) \leq 4mcds(G) + 1$. Later, Wu et al. [17] improved this ratio to 3.8 by proving that the neighborhood of any two adjacent nodes can contain at most 8 nodes. In [18], Gao et al. showed the bound can be at most 3.453 and Li et al. improved the ratio into 3.4305 in [19]. Recently, Du et al. [20] showed that $mis(G) \leq 3.399mcds(G) + 4.874$, which is the best result up to now.

To analyze the performance of those approximations, we need to decompose the algorithm selection and compare each part separately to an optimal solution. If $alg(G)$ is the size of selected MCDS by those algorithms, then the approximation ratio of these algorithms can be calculated by

$$\frac{alg(G)}{mcds(G)} = \frac{mis(G)}{mcds(G)} + \frac{connector(G)}{mcds(G)},$$

where $mis(G)$ is the size of MIS the algorithm selected, $connector(G)$ is the number of nodes used to connect such MIS, and $mcds(G)$ is the size of an optimal MCDS. Generally, $connector(G)$ highly depends on the value of $mis(G)$. Thus, the ratio $mis(G)/mcds(G)$ plays an important role when analyzing the performance of those approximations.

An interesting geometric property between an MIS and a MCDS will be helpful for us to calculate $mis(G)/mcds(G)$. For example, in UDG, if we shrink the radius of a disk from 1 to 0.5 for any vertices in the graph (denoted as small disks), and enlarge the radius of a disk from 1 to 1.5 for any vertices in an optimal MCDS (denoted as large disks), then any small disks will locate in the region formed by the union of MCDS large disks, and any two disks formed by two independent vertices will not intersect with each other. Fig. 1 shows such a scenario, where the red points denote a vertex in MCDS and blue points denote independent vertices. Hence, we can apply disk packing, namely how many disks with radius 0.5 the dominating areas of an MCDS can contain, to estimate the ratio of $mis(G)/mcds(G)$.

Although finding a minimum CDS in UBG is very similar as in UDG, the approximation analysis for UBG is much harder since the geometric properties in UBG are more complicated to analyze than in UDG. In UDG, the problem of "how many disks of the same size can a disk touch" is a foundation for disk packing [18–20]. Easy to see, when a disk touch two disks of the same size, the angle of those two touched disks to this touching disk is at least $\pi/3$. Therefore, we can easily figure out that a disk can touch $\frac{2\pi}{\pi/3} = 6$ disks of the same size. However, when it comes to three-dimension, the corresponding discussion is not that easy. In UBG, we can use the same ideas in UDG and replace those disks with corresponding spheres. Then, we can use sphere packing to estimate the ratio of $mis(G)/mcds(G)$ in UBG. Similarly, we should first solve the corresponding extended problem, "how many spheres of the same size can a sphere touch", which is well known as Gregory–Newton problem. However, this problem is so difficult that it has been a puzzle in literature until 1953 [21].

To the best of our knowledge, few papers studied the approximation ratio for MCDS problem in UBG. In the earlier stage, Hansen et al. [22] discussed the expected size of a CDS in a random UBG and compared the performance of existing algorithms. Later, Butenko and Ursulenko [23] proved that the ratio of $mis(G)/mcds(G)$ in UBG is at most 11 by using the well-known fact that a sphere can touch at most twelve spheres of the same size, which induced an approximation ratio of 22 for MCDS in UBG. Zhong et al. [24] claimed that such ratio could be reduced to 16. However, Kim et al. [1] pointed out and proved that both the algorithm and approximation analysis in [24] have problems. Zou et al. [25] further reduced this ratio to $13 + \ln 10$. Recently, Kim et al. [1] referred the idea in [17] and tried to answer how many independent points can be contained in two adjacent unit balls. Finally, they improved the ratio of $mis(G)/mcds(G)$ into 10.917 by showing

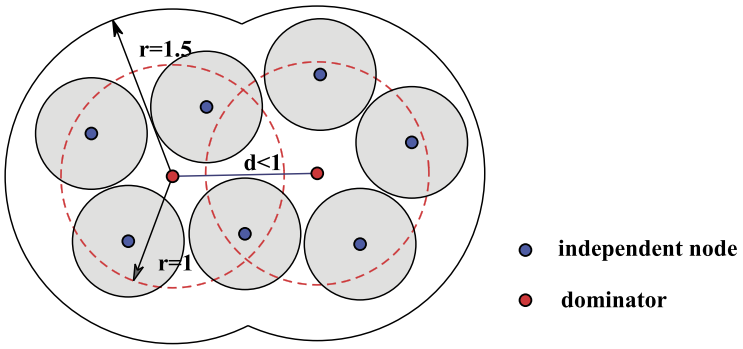

Fig. 1. An example to show disk packing.

that there are at most 22 independent points in two adjacent unit balls, and finally got an approximation ratio of MCDS as 14.937, which is the best result up to now.

However, after careful investigation, we find that during the deduction process in [1], one of the intermediate assertion is incorrect, which overthrows the final result completely. The main technique they implemented in their proof is a projection method to the ball surface and then applying some famous graph theories, and the problem comes under some scenarios when the projection result cannot guarantee the distance lower bound of two independent points. Researchers later found that designing a projection method to guarantee the distance lower bound is not an easy step, and it remains an open question in recent years [26]. As a consequence, in this paper we will first introduce a new projection method to guarantee the distance bound, and then illustrate the bound of $mis(G)/mcds(G)$ with some new analyzing techniques. Since the mistake in [1] only influences the analysis of the approximation ratio $mis(G)/mcds(G)$, the algorithms and analysis in the MIS connecting part in [1] remain to be correct. Thus we will adopt those correct parts to solve the MCDS problem completely. At the end of this paper, we will further optimize the algorithms for MCDS selection in [1] with prune process and validate the efficiency of our design by numerical experiments.

The rest of the paper is organized as follows: Section 2 illustrates the problem in [1] with counter examples. Section 3 introduces our new projection method to analyze the ratio of $mis(G)/mcds(G)$. Section 4 discusses how to improve MCDS algorithm while Section 5 exhibits the simulation results with different parameter settings. Finally, Section 6 summarizes this paper.

2. Independent points in two adjacent unit balls

In [17], Wu et al. first proved that the neighborhood of any two adjacent nodes can contain at most 8 nodes in UDG. Based on this fact, they then use mathematical induction to improve the ratio $mis(G)/mcds(G)$ to 3.8. Similar with the analysis in [17], once we have the answer of *"two-ball problem"*, we can deduce a better upper bound for the ratio $mis(G)/mcds(G)$ and reduce the overall approximation ratio. *Two-ball problem* means the problem of "how many independent points can be contained in two adjacent unit balls". Here two adjacent unit balls mean the Euclidean distance between two balls with unit radius is at most 1, while any two points are called independent points if and only if their Euclidean distance is at least 1.

Actually, what Kim et al. did in [1] follows this idea. However, their method have an unavoidable error. In Subsection 2.1 we will review their method to prove two-ball problem, and then in Subsection 2.2 we will precisely point out where their problem lies and provide a counter example to validate our claim.

2.1. Review Kim's method in [1]

In [1], Kim et al. referred the idea in [17] and improved the ratio of $mis(G)/mcds(G)$ into 10.917 by showing that there are at most 22 independent points in two adjacent unit balls. Their answer to the two-ball problem is the most important contribution in their paper. In order to solve the two-ball problem, Kim et al. extended the approach for solving the famous Gregory–Newton problem [21]. They considered two adjacent unit balls, say, B_1 and B_2 with centers u_1 and u_2. To get an upper bound of MIS in these two adjacent balls, they assumed that the Euclidean distance between u_1 and u_2 is equal to 1, since the total volume of $B_1 \cap B_2$ is larger when the distance between these two adjacent nodes increases, and consequently more independent nodes can be contained in $B_1 \cap B_2$. They then divided all the independent nodes into two categories: the nodes located in $(B_1 \cup B_2) \backslash (B_1 \cap B_2)$ and the nodes in $B_1 \cap B_2$. They mainly focused on the former part and claimed that the size of MIS in this region is at most 20 with a special "projection" method.

Their projection method is a mapping rule to project all the independent nodes in $(B_1 \cup B_2) \backslash (B_1 \cap B_2)$ to the surface of $B_1 \cup B_2$. The detailed description can be shown as follows: For each independent node v, if $v \in B_1 \backslash B_2$ (respectively, $B_2 \backslash B_1$), then draw a radial from u_1 (respectively, u_2) going through v, and intersect the outer surface of B_1 (denoted by $Sur(B_1)$,

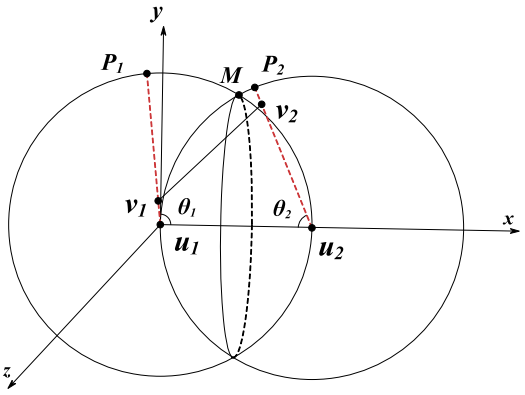

Fig. 2. An example to show $d(P_1, P_2) < 1$.

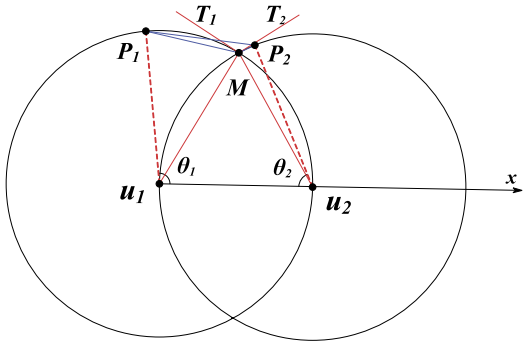

Fig. 3. A counter example in 2D.

and respectively $Sur(B_2)$) at point P. By this mapping rule, they got the projection points set $\{P_1, P_2, \cdots, P_t\}$, where t is the size of MIS in $(B_1 \cup B_2)\backslash(B_1 \cap B_2)$.

Next, for any two points P_i and P_j, if their Euclidean distance (denoted by $d(P_i, P_j)$) is between 1 and $3\arccos(1/7)\pi$, they made a curve from P_i to P_j on $Sur(B_1 \cup B_2)$ in the specified way as shown in Section 3.2.1 in [1]. These curves partition $Sur(B_1 \cup B_2)$ into some tiny faces. By analyzing the lower bounds of those faces' areas and using Euler's formula, they proved that $t \leq 20$. Combined with the fact that a unit ball can pack at most 12 independent nodes [21], they finally concluded that the number of MIS in the union of two adjacent unit balls is at most 22.

2.2. The problem of Kim's method with counter examples

After careful investigation, we find that in Section 3.2 of [1], one of the intermediate assertion is incorrect, which overthrows the final result completely. This assertion says:

> "According to their mapping rule, on $Sur(B_1 \cup B_2)$, for any P_i and P_j, $d(P_i, P_j) > 1$."

The assertion is a foundation of their work. With this assertion, they could conclude that no two curves on $Sur(B_1 \cup B_2)$ can intersect, which is a declaration to guarantee the correctness of the lower bound for the tiny faces' areas on $Sur(B_1 \cup B_2)$.

However, although in many cases this assertion seems correct, it is not valid for every possible scenario. Let us provide an example to show why it is incorrect. In this example, v_1 and v_2 are two independent nodes located in two different balls and their projection points are P_1 and P_2 respectively, as Fig. 2 shows. Specially, we can let v_1, v_2, u_1 and u_2 locate in a same plane. Moreover, we set $\theta_1 + \theta_2 \leq \pi$, where θ_1, θ_2 denote $\angle v_1u_1u_2$ and $\angle v_2u_2u_1$ respectively.

Now we prove that $d(P_1, P_2) \leq 1$ in this situation. Since all points in this case are on a same plane, we can convert this case as a 2D plane in Fig. 3. Consider ΔP_1MP_2 in Fig. 3, by the Law of Cosines, we have

$$d^2(P_1, P_2) = d^2(P_1, M) + d^2(M, P_2) - 2d(P_1, M)d(M, P_2)\cos\angle P_1MP_2.$$

From Fig. 3, we find that

$$\angle P_1MP_2 = \angle T_1MT_2 + \angle T_1MP_1 + \angle T_2MP_2, \text{ where } \angle u_1MT_1 = \angle u_2MT_2 = \pi/2.$$

Table 1
Notations and symbols.

Notation	Description
$d(P, Q)$	The Euclidean distance between P and Q
$\|PQ\|$	The spherical distance between P and Q on a ball or the arc distance on a disk
u_1 and u_2	Two "constant" dominator nodes in this section, and $d(u_1, u_2) = 1$
B_1 and B_2	Two adjacent unit balls with centers u_1 and u_2
$Sur(B)$	The outer surface of a geometric object B
$disk(v)$	The unit disk with center v
L	The intersection of the perpendicular bisector plane of segment u_1u_2 with $Sur(B_1 \cup B_2)$
direct projection	The mapping rule in [1] (as mentioned in Section 2.1)
$dpp(v)$	The direct projection point of v
principal plane	For any vertex v, the plane going through point v, u_1 and u_2 is called the principal plane of v
$pp(v)$	The principal plane of v

Here T_1M and T_2M are tangent lines to $disk(u_1)$ and $disk(u_2)$ respectively ($disk(u)$ is the cycle centered at u with radius 1). According to Alternate Segment Theorem,

$$\angle T_1MP_1 = \angle P_1u_1M/2,\ \angle T_2MP_2 = \angle P_2u_2M/2.$$

Therefore, $\angle P_1MP_2 = (\theta_1 + \theta_2)/2 + \pi/3$. Also, it is easy to get $\angle P_1u_1M = \theta_1 - \pi/3$. Then,

$$d(P_1, M) = 2\sin(\theta_1/2 - \pi/6),\ d(P_2, M) = 2\sin(\theta_2/2 - \pi/6).$$

Hence, the Euclidean distance between P_1 and P_2 is:

$$d^2(P_1, P_2) = 4\cos^2(\frac{\theta_1 + \theta_2}{2}) - 4\cos(\frac{\theta_1 + \theta_2}{2})\cos(\frac{\theta_1 - \theta_2}{2}) + 1.$$

Since $\theta_1 + \theta_2 \le \pi$ in this case, $0 \le \cos(\frac{\theta_1 + \theta_2}{2}) \le \cos(\frac{\theta_1 - \theta_2}{2})$. Therefore, $d^2(P_1, P_2) \le 1$, which is a counter example for Kim's assertion.

Actually, we can also get a lower bound for $d(P_1, P_2)$ when v_1 and v_2 move to points u_1 and M respectively. In that case, $d(P_1, P_2)$ is equal to $2\sin(\pi/12) \approx 0.5176$, which is far less than 1.

Correspondingly, if we cannot ensure the distance between any two projection vertices P_i and P_j is always larger than 1, then the two diagonals of the quadrilateral formed by four projection points can be both smaller than $3\arccos(1/7)/\pi$. In that case, the two diagonal curves will intersect. Hence, the correctness of the work in [1] meets great difficulty.

3. A new projection method

According to the discussion in Subsection 2.2, we have to guarantee $d(P_1', P_2') \ge 1$ for any pair of independent points on the surface of two adjacent unit balls if we hope to achieve an approximation ratio of 10.917. In this section we introduce a new projection method to overcome Kim's flaw. The main idea of our method is an adaptive jitter scheme in the projection process when we map the independent nodes in $(B_1 \cup B_2)\backslash(B_1 \cap B_2)$ to the surface of $B_1 \cup B_2$.

In detail, we first propose Lemma 1 to show that every projection point in [1] has an available range (and we define it as Effective Projection Region). Arbitrarily moving any two projection points in their Effective Projection Region will not break the condition $d(P_1', P_2') \ge 1$ if the projection points are located in a same ball. The next part of this section is to prove the same property for the case where the projection points are located in different balls. Correspondingly, we formally define our new projection in Definition 4. With this new projection, we have Theorem 5, which is our main observation in this section. To make the proof of Theorem 5 better understood, we first discuss the two-dimensional situation as a special case in Subsection 3.1. Afterwards, we generalize our conclusion for three-dimensional situation in Subsection 3.2. With Theorem 5, we can use our new projection to replace the projection in [1] and use the remaining part in [1] to correctly achieve an approximation ratio of 10.917 for $mis(G)/mcds(G)$.

Before introducing our new projection, we need to introduce some notations and definitions as Table 1 shows, which are frequently used in the rest of this paper.

In order to apply geometric principle to solve our problem, we allow that the distance between a pair of independent nodes is equal to one, which is also the densest case. (Actually, we will often use this critical distance in the coming parts of analysis.) Also, as discussed before, to get an upper bound of MIS in two adjacent balls, we should make the Euclidean distance between them as large as possible. Thus as Table 1 shows, we set $d(u_1, u_2) = 1$.

In most cases, for any two independent nodes v_1, v_2 located in B_1 and B_2 respectively, we know that $d(P_1, P_2)$ is larger than 1, where $P_1 = dpp(v_1)$ and $P_2 = dpp(v_2)$. However, sometimes $d(P_1, P_2)$ may be also less than 1 as Subsection 2.1 shows. According to our observation, when $d(P_1, P_2) < 1$ occurs, at least one of v_1 and v_2 is much closer to its dominator (u_1 or u_2), which can be found from Fig. 2. Without loss of generality, we say the closer node is v_1. In the unit ball B_1, we know the size of its MIS is at most 12. But if we want to put all the 12 independent nodes in B_1, the efficient way is to put

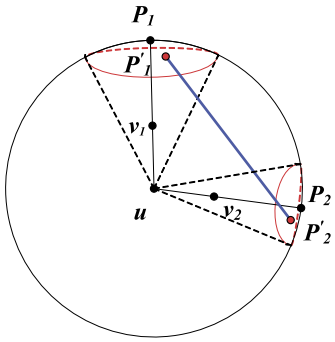

Fig. 4. The new projection of P'_1 and P'_2.

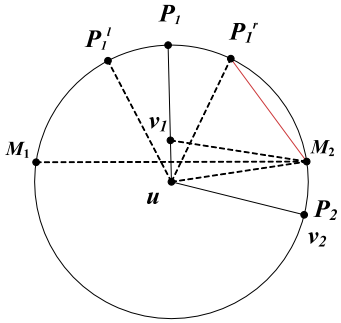

Fig. 5. The projection region when $r_2 = 1$.

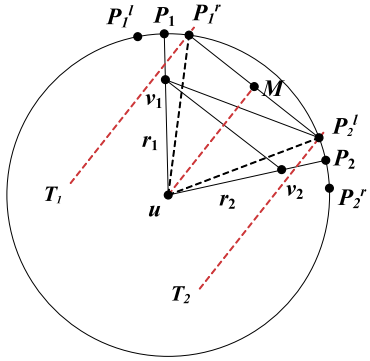

Fig. 6. The projection region when $r_2 < 1$.

all of them on $Sur(B_1)$. Consequently, if v_1 is much closer to u_1, it will greatly affect the total number of MIS in B_1, and the size of MIS in $B_1 \cup B_2$ will also be affected. We consider this MIS number decrease as the sacrifice to shorten $d(P_1, P_2)$. In order to quantitatively describe and use this property, we provide Lemma 1 as follows.

Lemma 1. *A unit ball B with center u contains two independent points v_1, v_2 and $d(u, v_1) = r_1$, $d(u, v_2) = r_2$, $dpp(v_1) = P_1$, $dpp(v_2) = P_2$. P'_1 (respectively, P'_2) is an arbitrary point in the cycle region on $Sur(B_1)$ (respectively, $Sur(B_2)$) with center P_1 (respectively, P_2) and spherical radius* $\arccos(r_1/2) - \pi/3$ *(respectively,* $\arccos(r_2/2) - \pi/3$*) as Fig. 4 shows. Then $d(P'_1, P'_2) \geq 1$.*

Proof. First, we consider the 2D situation as Figs. 5 and 6 show. In Fig. 5, point v_1 is in $disk(u)$. M_1, M_2 are intersection points of uv_1' perpendicular bisector and $disk(u)$. Since all independent nodes with v_1 are outside $disk(v_1)$, nodes in $disk(u)$ which are independent with v_1 cannot locate above line M_1M_2.

It is easy to know the available region of P'_1 on $disk(u)$ is from P_1^l to P_1^r, where $|P_1^l P_1| = |P_1 P_1^r| = \arccos(r_1/2) - \pi/3$ (shown in Fig. 5). Further, $\angle M_2 u v_1 = \arccos(r_1/2)$. Hence, $|P_1^r M_2| = \pi/3$ and $d(P_1^r, M_2) = 1$. Similarly, $d(P_1^l, M_1) = 1$. Based on the location of v_2, there are two situations to discuss.

Case 1: If v_2 is on the circle of $disk(u)$, then P_2, P_2' and v_2 are the same point. Since v_2 must locate below M_1M_2 and P_1' is on the arc between P_1^l and P_1^r, it is obvious to conclude that $d(P_1'P_2') \geq 1$.

Case 2: When v_2 is not on the circle of $disk(u)$ (as Fig. 6 shows), P_1' (P_2', respectively) locates between P_1^l and P_1^r (P_2^l and P_2^r, respectively). Next, we will prove that $d(P_1', P_2')$ is minimum when P_1' is at point P_1^r and P_2' is at point P_2^l.

As Fig. 6 shows, segment uM is the midperpendicular of $P_1^rP_2^l$. And lines $P_1^rT_1$ and $P_2^lT_2$ are parallel to uM. Then, all points in the arc from P_1^l to P_1^r and the arc from P_2^l to P_2^r are outside the parallel lines $P_1^rT_1$ and $P_2^lT_2$. Therefore, $d(P_1', P_2') \geq d(P_1^rP_2^l)$. On the other side, $d(P_1^rP_2^l) \geq 1$ is equivalent to $\left|P_1^rP_2^l\right| \geq \pi/3$. Combining with Law of Cosines, we have

$$\left|P_1^rP_2^l\right| = \angle P_1^rP_2^l = \angle P_1uP_2 - \angle P_1uP_1^r - \angle P_2uP_2^l = \arccos\left(\frac{r_1^2+r_2^2-1}{2r_1r_2}\right) - \left[\arccos\left(\frac{r_1}{2}\right) - \pi/3\right] - \left[\arccos\left(\frac{r_2}{2}\right) - \pi/3\right].$$

When r_1 is fixed, it can be proved that the value of $\left|P_1^rP_2^l\right|$ decreases when r_2 increases.

Let $f(r_1, r_2) = \arccos(\frac{r_1^2+r_2^2-1}{2r_1r_2}) - [\arccos(\frac{r_1}{2}) - \frac{\pi}{3}] - [\arccos(\frac{r_2}{2}) - \frac{\pi}{3}]$. Then,

$$\frac{\partial f(r_1,r_2)}{\partial r_2} = \frac{1}{2}\frac{1}{\sqrt{1-(\frac{r_2}{2})^2}} - \frac{r_2^2-r_1^2+1}{2r_2^2r_1}\frac{1}{\sqrt{1-(\frac{r_2^2+r_1^2-1}{2r_2r_1})^2}} = \frac{1}{2}\frac{1}{\sqrt{1-(\frac{r_2}{2})^2}} - \frac{r_2^2-r_1^2+1}{2r_2^2}\frac{1}{\sqrt{r_1^2-(\frac{r_2^2+r_1^2-1}{2r_2})^2}}.$$

Since $r_1 \leq 1$, $\frac{r_2^2+1-r_1^2}{2r_2^2} \geq \frac{1}{2}$. Moreover,

$$1-\left(\frac{r_2}{2}\right)^2 \geq r_1^2 - \left(\frac{r_2^2+r_1^2-1}{2r_2}\right)^2 \Leftrightarrow r_1^2 - 1 \leq 2r_2^2.$$

Obviously, $r_1^2 - 1 \leq 0 \leq 2r_2^2$. Therefore, $\frac{\partial f(r_2)}{\partial r_2} \leq 0$, which means $f(r_2)$ decreases with the value of r_2 increases.

Thus, when r_2 equals one, $\left|P_1^rP_2^l\right|$ will be minimized, which is exactly **Case 1** where v_2 is on the circle of $disk_1(u)$. Hence, $d(P_1', P_2') \geq 1$.

Similarly, it is easy to extend the 2-dimensional situation to 3-dimensional situation. In this situation, u, v_1, v_2, P_1 and P_2 are in the same plane. In this plane, there also exist a pair of boundary points (P_1^r, P_1^l, P_2^l, P_2^r) for P_1' and P_2' on the big circle going through u, v_1, and v_2. We can also draw two planes respectively going through P_1^r and P_2^l and make them parallel to the midperpendicular plane of segment $P_1^rP_2^l$. It is easy to see that points P_1' and P_2' will not locate inside those two parallel planes. Therefore, $d(P_1', P_2') \geq d(P_1^r, P_2^l) \geq 1$, which has been proved in 2-dimensional situation. □

According to Lemma 1, we come up with a new region called "Effective Projection Region" to describe the extra feasible moving space of P_1' or P_2'.

Definition 2 *(Effective projection region).* For node v in a unit ball B, its direct projection point is P. The region on $Sur(B)$ whose center is point P and spherical radius is $\arccos(r/2) - \pi/3$ is called v's effective projection region, where r is the Euclidean distance between v and B's center.

Obviously, in a 3D space, for any two independent nodes v_1 and v_2 in a unit ball B, their direct projection points are P_1 and P_2. According to Lemma 1, if we arbitrarily move P_1 and P_2 along $Sur(B)$ inside their effective projection regions, $d(P_1, P_2)$ will always ≥ 1. Next, we will discuss the situation where v_1 and v_2 are in two different balls. Before that, we first define our new projection rule.

Definition 3 *(Region projection).* For any independent node v, its direct projection point is P, then any point which locates in v's effective projection region is a Region Projection point of v.

Definition 4 *(Final projection).* For any point v in $(B_1 \cup B_2)\backslash(B_1 \cap B_2)$, the $pp(v)$ intersects with L and we assume M is the closer intersection point to v. P' is v's final projection if and only if it satisfies conditions as follows:

1) P' is a region projection point of v.
2) P' is located on $pp(v)$.

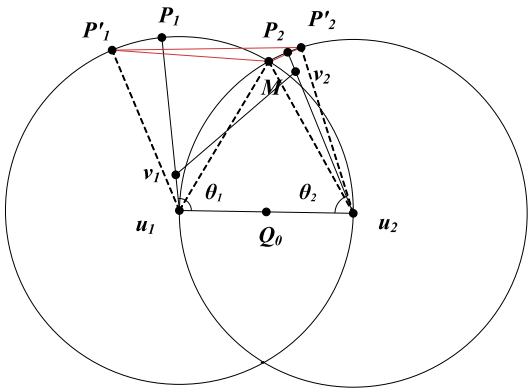

Fig. 7. Discussion in 2-dimensional space.

3) Among all the points satisfying 1) and 2), P' is the farthest from M.

Theorem 5. *For any two independent nodes v_1 and v_2 in $(B_1 \cup B_2)\backslash(B_1 \cap B_2)$, their final projection points are P'_1 and P'_2. Then, $d(P'_1, P'_2) \geq 1$.*

Next, we will prove the correctness of Theorem 5. To make it simple, we first discuss the two-dimensional situation as a special case in Subsection 3.1. Afterwards, we generalize our conclusion for three-dimensional situation in Subsection 3.2.

By Lemma 1, if v_1 and v_2 are in the same unit ball, $d(P'_1, P'_2) \geq 1$. Thus, we only need to consider the situation when v_1, v_2 are in different balls. Without loss of generality, let v_1 in B_1 and v_2 in B_2.

3.1. Proof of Theorem 5 in 2-dimensional space

When u_1v_1 and u_2v_2 are in the same principal plane, our problem turns into a 2D problem as shown in Fig. 7.

In Fig. 7, P_1 and P_2 denote $dpp(v_1)$ and $dpp(v_2)$; θ_1 and θ_2 denote $\angle P_1u_1u_2$ and $\angle P_2u_2u_1$; r_1 and r_2 denote $d(v_1, u_1)$ and $d(v_2, u_2)$; α and β denote $\left|P'_1M\right|$ and $\left|P'_2M\right|$ respectively. M is the intersection of the common principal plane with L. To simplify our problem, we assume $d(v_1, v_2) = 1$.

As we did in Section 2.2, we can figure out the expression of $d(P'_1, P'_2)$. In $\Delta P'_1MP'_2$, it is easy to figure out that

$$d(P'_1, M) = 2\sin\frac{\alpha}{2}, d(P'_2, M) = 2\sin\frac{\beta}{2}, \text{ and } \angle P'_1MP'_2 = \frac{2\pi}{3} + \frac{\alpha+\beta}{2},$$

(with Alternate Segment Theorem). By the Law of Cosines, we have

$$\begin{aligned} d^2(P'_1, P'_2) &= \left(2\sin\frac{\alpha}{2}\right)^2 + \left(2\sin\frac{\beta}{2}\right)^2 - 2\left(2\sin\frac{\alpha}{2}\right)\left(2\sin\frac{\beta}{2}\right)\cos\angle P'_1MP'_2 \\ &= 4\cos^2\left(\frac{\alpha+\beta}{2} + \frac{\pi}{3}\right) - 4\cos\left(\frac{\alpha+\beta}{2} + \frac{\pi}{3}\right)\cos\left(\frac{\alpha-\beta}{2}\right) + 1. \end{aligned} \tag{1}$$

Let $x = \cos(\frac{\alpha+\beta}{2} + \frac{\pi}{3})$ and $y = \cos(\frac{\alpha-\beta}{2})$. Construct function $f(x, y) = 4x^2 - 4yx + 1$, where $y \geq 0$. Easy to see that $x \leq 0 \Rightarrow f(x, y) \geq 1$. That means $\alpha + \beta \geq \frac{\pi}{3}$. Moreover,

$$f(x, y) \geq 1 \Leftrightarrow x \leq 0 \quad \text{or} \quad x \geq y.$$

If $x \geq y$, then $\cos(\frac{\alpha+\beta}{2} + \frac{\pi}{3}) \geq \cos(\frac{\alpha-\beta}{2}) \geq 0$. Hence, $\alpha + \beta \leq \frac{\pi}{3}$ and $\frac{\alpha+\beta}{2} + \frac{\pi}{3} \leq \frac{\alpha-\beta}{2} \Rightarrow \beta + \frac{\pi}{3} \leq 0$, which is impossible. Therefore, $d(P'_1, P'_2) \geq 1$ is equivalent to $\alpha + \beta \geq \frac{\pi}{3}$.

According to Definition 4, we have $\alpha = \theta_1 + \arccos(r_1/2) - 2\pi/3$, and $\beta = \theta_1 + \arccos(r_1/2) - 2\pi/3$. Thus, our goal is to prove

$$\theta_1 + \theta_2 + \arccos(\frac{r_1}{2}) + \arccos(\frac{r_2}{2}) \geq \frac{5\pi}{3}. \tag{2}$$

As $\arccos(r_1/2) \geq \pi/3$ and $\arccos(r_2/2) \geq \pi/3$, we only need to consider the case where $\theta_1 + \theta_2 < \pi$. Based on this, we have Lemma 6.

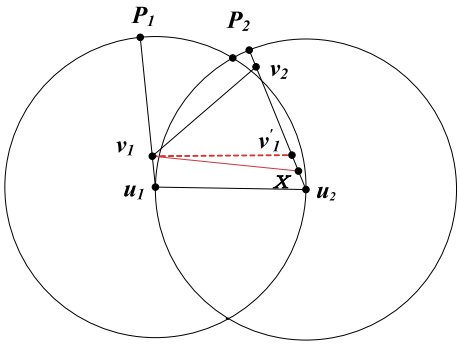

Fig. 8. Proof of $d(v_1, P_2) \geq 1$.

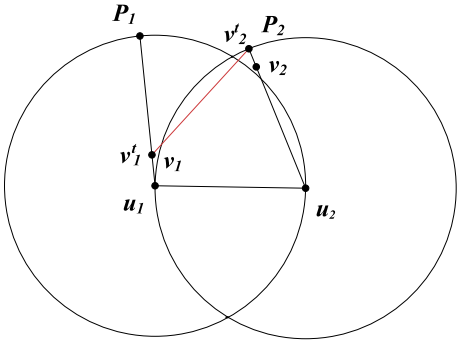

Fig. 9. The transitive instance.

Lemma 6. *At least one of $d(v_1, P_2)$ and $d(v_2, P_1)$ is equal to or larger than 1.*

Proof. Since $d(v_1, v_2) = 1$ and $\theta_1 + \theta_2 < \pi$, v_1v_2 can not be parallel to u_1u_2. Without loss of generality, assume v_1 is closer to u_1u_2, as Fig. 8 shows.

Draw a line $v_1v'_1$, make it parallel to u_1u_2 and intersect with u_2v_2 on point v'_1. Since $\theta_1 + \theta_2 < \pi$, $v_1v'_1 < 1$, there must exist a point X between u_2 and v'_1 such that $d(v_1, X) = 1$. Hence, $\angle v_1v_2u_2 < \pi/2$. Consequently, $d(v_1, P_2) \geq d(v_1, v_2) = 1$. □

In our problem, the value of $d(P'_1, P'_2)$ completely depends on parameters: r_1, r_2, θ_1, and θ_2. Once these four parameters are given, the value of $d(P'_1, P'_2)$ is completely specified. Therefore, we use $(r_1, r_2, \theta_1, \theta_2)$ to denote one instance of our problem.

Lemma 7. *For any fixed instance $(r_1, r_2, \theta_1, \theta_2)$ with $d(v_1, v_2) = 1$, there always exists an instance $(r'_1, 1, \theta'_1, \theta'_2)$ or $(1, r'_2, \theta'_1, \theta'_2)$ with $d(v'_1, v'_2) = 1$ such that $d(P'_1, P'_2)$ in the former instance is larger than the later one.*

Proof. To prove this lemma, we need to construct a transformation from the original instance $(r_1, r_2, \theta_1, \theta_2)$ to the destination instance $(r'_1, 1, \theta'_1, \theta'_2)$ or $(1, r'_2, \theta'_1, \theta'_2)$. According to Lemma 6, we assume that in the original instance $d(v_1, P_2) \geq 1$ without loss of generality.

Let us consider a transitive instance $(r_1, 1, \theta_1, \theta_2)$, as Fig. 9 shows. In this transitive instance, v^t_1 and v^t_2 are the two independent nodes and they locate on v_1 and P_2 respectively. Compared with the original instance, this transitive instance owns a same α and a smaller β. Consequently, $d(P'_1, P'_2)$ in transitive instance is shorter than the original instance.

Next, we will construct the destination instance from the transitive instance. As Fig. 10 shows, we put v'_2 on the point v^t_2. $disk(v'_2)$ intersects with segments u_1P_1 and $v^t_1v^t_2$ on F_1 and F_2. Then we put v'_1 on the arc between F_1 and F_2 and make sure v'_1 locates outside $disk(u_2)$. It is easy to verify that $\angle v'_1u_1u_2 \leq \angle v_1u_1u_2$ and $d(v'_1, u_1) \geq d(v_1, u_1)$ which results in a smaller α. Consequently, $d(P'_1, P'_2)$ is also smaller.

In conclusion, Lemma 6 follows. □

Since we want to explore the minimum value of $d(P'_1, P'_2)$, we will use $(r_1, 1, \theta_1, \theta_2)$ with $d(v_1, v_2) = 1$ to complete our next work.

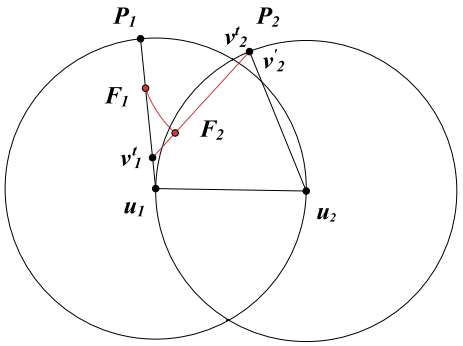

Fig. 10. The construction of destination instance.

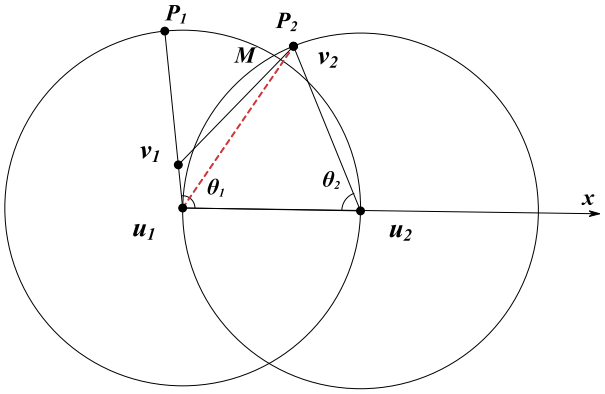

Fig. 11. The value of r_1 in 2-dimensional space.

Since $d(v_1, v_2) = 1$, we can figure out the relation between θ_1 and r_1, θ_2. As Fig. 11 shows, we build a polar coordinates on u_1. In $\Delta v_2 u_1 u_2$, it is easy to figure out that $d(v_2, u_1) = 2\sin(\theta_2/2)$. Then, the coordinates of v_1 and v_2 are (θ_1, r_1) and $(\pi/2 - \theta_2/2, 2\sin(\theta_2/2))$. Hence, we have

$$d^2(v_1, v_2) = r_1^2 + \left(2\sin\frac{\theta_2}{2}\right)^2 - 2r_1\left(2\sin\frac{\theta_2}{2}\right)\cos\left(\theta_1 - \frac{\pi - \theta_2}{2}\right) = 1$$

$$\Rightarrow \sin\left(\theta_1 + \frac{\theta_2}{2}\right) = \frac{r_1^2 - 1 + 4\sin^2\frac{\theta_2}{2}}{4r_1\sin\frac{\theta_2}{2}}$$

Since $\theta_1, \theta_2 \in [\pi/3, 2\pi/3]$, then $\theta_1 + \theta_2/2 \geq \pi/2$. Hence,

$$\theta_1 = \pi - \frac{\theta_2}{2} - \arcsin\left(\frac{r_1^2 - 1 + 4\sin^2\frac{\theta_2}{2}}{4r_1\sin\frac{\theta_2}{2}}\right). \tag{3}$$

With Equation (3), the value of $|P_1'M|$ is a function of r_1 and θ_2, and we denote it as $\alpha(r_1, \theta_2)$. According to Definition 4, we have

$$\alpha(r_1, \theta_2) = \pi - \frac{\theta_2}{2} - \arcsin\left(\frac{r_1^2 - 1 + 4\sin^2\frac{\theta_2}{2}}{4r_1\sin\frac{\theta_2}{2}}\right) + \arccos(\frac{r_1}{2}) + \frac{2\pi}{3}.$$

By analyzing the sign of $\partial\alpha(r_1, \theta_2)/\partial r_1$, it can be proved that, when θ_2 is fixed, $\alpha(r_1, \theta_2)$ is minimum when r_1 is minimum or maximal. Since all we talk here is a special case of 3-dimensional situation, the detailed proof can be found in Lemma 10. Therefore, what we need to do next is to verify $d(P_1', P_2') \geq 1$ for the two situations where r_1 is minimal and maximal.

Case 1: (r_1 **is minimal):** For this case, we first need to figure out the minimal value of r_1 when θ_2 is fixed. Considering v_1 locates in $disk(u_1)\backslash disk(u_2)$, it is obvious that, when v_1 locates on the intersection of $disk(v_2)$ with $disk(u_2)$, r_1 reaches minimal. Then, $d(v_1, u_2) = 1$, $\angle v_1 u_2 v_2 = \pi/3$, $\theta_1 = 2\pi/3 - \theta_2/2$ and $r_1 = 2\cos\theta_1$. Consequently, $\theta_1 + \theta_2 + \arccos(r_1/2) + \arccos(r_2/2) = 5\pi/3$ which meets inequality (2). Hence, in this case, $d(P_1', P_2') \geq 1$.

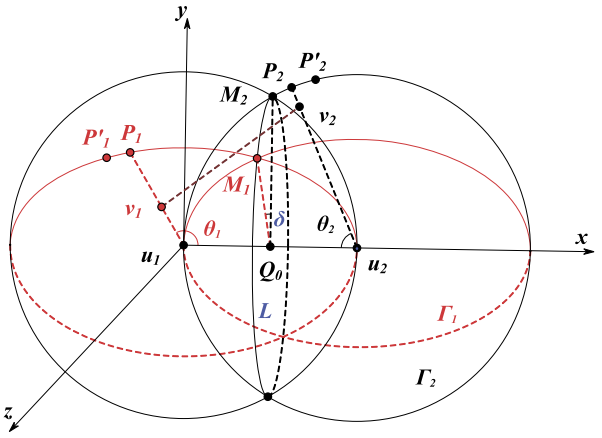

Fig. 12. Discussion in 3-dimensional space.

Case 2: (r_1 **is maximal):** It is easy to figure out that the maximal value of r_1 is 1 when v_1 locates on the boundary of $disk(u_1)$. In this case, P'_1 and v_1 are the same. $d(P'_1, P'_2) = d(v_1, v_2) = 1$ which also meets the requirement in Theorem 5.

Now that statement of Theorem 5 holds for the two above situations where $d(P'_1, P'_2)$ will reach the minimal, Theorem 5 holds for any case in 2-dimensional space.

3.2. Proof of Theorem 5 in 3-dimensional space

In this section, we discuss the general situation where u_1v_1 and u_2v_2 are in different principal planes. In this case, we follow the ideas in 2-dimensional situation and give the same result.

First we explore the equivalent condition for $d(P'_1, P'_2) \geq 1$. In Fig. 12, δ denotes the dihedral angle between those two principal planes, Γ_1 and Γ_2; α and β denote $\left|P'_1M_1\right|$ and $\left|P'_2M_2\right|$ respectively. Similar as analysis in Section 3.1, we have $d(P'_1, M) = 2\sin\frac{\alpha}{2}$, and $d(P'_2, M) = 2\sin\frac{\beta}{2}$. Using method of analytical geometry, we have

$$\begin{aligned} d^2(P'_1, P'_2) = {} & 4\cos^2\left(\frac{\alpha+\beta}{2}+\frac{\pi}{3}\right) - 4\cos\left(\frac{\alpha+\beta}{2}+\frac{\pi}{3}\right)\cos\left(\frac{\alpha-\beta}{2}\right)+1 \\ & + \left[\cos(\alpha-\beta) - \cos\left(\alpha+\beta+\frac{2\pi}{3}\right)\right](1-\cos\delta). \end{aligned} \tag{4}$$

Note that, when $\delta = 0$, Equation (4) turns to Equation (1). Since positive δ also contributes to $d(P'_1, P'_2)$ from Equation (4), then $d(P'_1, P'_2)$ will be definitely larger than 1 when $\theta_1 + \theta_2 > \pi$. Therefore, we still just need to consider the situation where $\theta_1 + \theta_2 < \pi$.

Let $x = \cos((\alpha+\beta)/2 + \pi/3)$, $y = \cos(\alpha-\beta)/2$, and $z = \cos\delta$. Thus,

$$d^2(P'_1, P'_2) = 2(1+z)x^2 - 4yx + 2(1-z)y^2 + 1.$$

Construct function $g(x, y) = 2(1+z)x^2 - 4yx + 2(1-z)y^2 + 1$. It is easy to find the solution of inequality $g(x, y) \geq 1$ and its effective solution is

$$\frac{x}{y} \leq \frac{1-z}{1+z}. \tag{5}$$

Hence, $d(P'_1, P'_2) \geq 1$ is equivalent to Equation (5).

Next, we will show some lemmas as we did in Section 3.1.

Lemma 8. *Let φ_1 and φ_2 denote $\angle v_2v_1u_1$ and $\angle v_1v_2u_2$. Then, at least one of them is at most $\pi/2$. Moreover, at least one of $d(v_1, P_2)$ and $d(v_2, P_1)$ is equal to or larger than 1.*

Proof. Here, we prove it by contradiction. We assume that both φ_1 and φ_2 are greater than $\pi/2$. In $\Delta v_1u_1v_2$ and $\Delta u_2u_1v_2$, using the Law of Cosines, we have

$$\begin{aligned} d^2(u_1, v_2) &= d^2(v_1, v_2) + d^2(u_1, v_1) - 2d(v_1, v_2)d(u_1, v_1)\cos\varphi_1 \\ &= d^2(u_2, v_2) + d^2(u_1, u_2) - 2d(u_2, v_2)d(u_1, u_2)\cos\theta_2. \end{aligned}$$

Hence, we have

$$\cos\varphi_1 = \frac{r_1^2 - r_2^2 + 2r_2\cos\theta_2}{2r_1}.$$

Similarly,

$$\cos\varphi_2 = \frac{r_2^2 - r_1^2 + 2r_1\cos\theta_1}{2r_2}.$$

Since $\varphi_1 > \pi/2$ and $\varphi_2 > \pi/2$, we have

$$\begin{cases} r_1^2 - r_2^2 + 2r_2\cos\theta_2 < 0 \\ r_2^2 - r_1^2 + 2r_1\cos\theta_1 < 0. \end{cases} \tag{6}$$

From Inequality (6), we can deduce that

$$r_1\cos\theta_1 + r_2\cos\theta_2 < 0. \tag{7}$$

Since we still have $\theta_1 + \theta_2 < \pi$, then $\cos\theta_1 + \cos\theta_2 > 0$. Also, $r_1 \le 1$ and $r_2 \le 1$. Therefore, we can assert that, for θ_1 and θ_2, one of them is $\ge \pi/2$ and the other is $\le \pi/2$. Without loss of generality, we assume $\theta_1 \ge \pi/2$. Then we have $\theta_2 \le \pi/2$. From inequality (7), we have

$$r_1(\cos\theta_1 + \cos\theta_2) + (r_2 - r_1)\cos\theta_2 < 0.$$

Since $r_1(\cos\theta_1 + \cos\theta_2) \ge 0$ and $\cos\theta_2 \ge 0$, then we have $r_1 > r_2$. In this case, $\cos\varphi_1$ will be equal to or larger than 0 which contradicts with our assumption. Hence, Lemma 8 holds. □

Lemma 9. *When δ is given, the maximal value of α (or β) we need to consider is* $2\arctan\left(\frac{1-2\tan^2(\delta/2)}{\sqrt{3}}\right)$.

Proof. In order to figure out the maximal value of α (or β) we need to consider in the next analysis, we think about the critical state of Inequality (5), which means

$$\frac{x}{y} = \frac{1-z}{1+z}.$$

Besides, this critical state also means $d(P_1', P_2') = 1$. In this case, β reaches maximal when $\alpha = 0$. We denote it with β_{max}. It is easy to figure out that $x = \cos(\beta_{max}/2 + \pi/3)$, $y = \cos(\beta_{max}/2)$ and $z = \cos\delta$. Therefore,

$$\frac{x}{y} = \frac{\cos\left(\frac{\beta_{max}}{2} + \frac{\pi}{3}\right)}{\cos\left(\frac{\beta_{max}}{2}\right)} = \frac{1}{2} - \frac{\sqrt{3}}{2}\tan\frac{\beta_{max}}{2}.$$

Besides,

$$\frac{1-z}{1+z} = \frac{1-\cos\delta}{1+\cos\delta} = \tan^2\left(\frac{\delta}{2}\right).$$

Then, it is easy to conclude that Lemma 9 holds. □

Similarly, we can use $(\delta, r_1, r_2, \theta_1, \theta_2)$ to denote one instance of our problem. According to Lemma 8, we can conclude that at least one of $d(v_1, P_2)$ and $d(v_2, P_1)$ is at least 1. Without loss of generality, we assume $d(v_1, P_2) \ge 1$. Similar as the analysis in the Section 3.1, we can verify that Lemma 7 could also be extended to three-dimensional situation here. Therefore, we use instance of $(\delta, r_1, 1, \theta_1, \theta_2)$ with $d(v_1, v_2) = 1$ to explore the lower value of $d(P_1', P_2')$.

Lemma 10. *For instance $(\delta, r_1, 1, \theta_1, \theta_2)$ with $d(v_1, v_2) = 1$, when δ and θ_2 are fixed, α is minimum when r_1 is minimum or maximal.*

Proof. When δ, θ_2 are fixed, we can figure out the relation between θ_1 and r_1 as we did in the Section 3.1. As Fig. 13 shows, we build rectangular coordinate systems $x - u_1 - y_1$ and $x - u_1 - y_2$ on Γ_1 and Γ_2 respectively, where Γ_1 and Γ_2 denote $pp(v_1)$ and $pp(v_2)$ respectively. Assuming the projection point of v_2 on $x - u_1 - y_1$ is v_2^p, it can be calculated that its coordinate in $x - u_1 - y_2$ is $(1 - \cos\theta_2, \sin\theta_2\cos\delta)$. The coordinate of v_1 in $x - u_1 - y_2$ is $(r_1\cos\theta_1, r_1\sin\theta_1)$. Then, it is easy to figure out that $d(v_2, v_2^p) = \sin\theta_2\sin\delta$ and $d(v_2, u_1) = 2\sin\frac{\theta_2}{2}$. Let μ and ρ denote $d(v_2^p, v_1)$ and $d(v_2^p, u_1)$ respectively. Then,

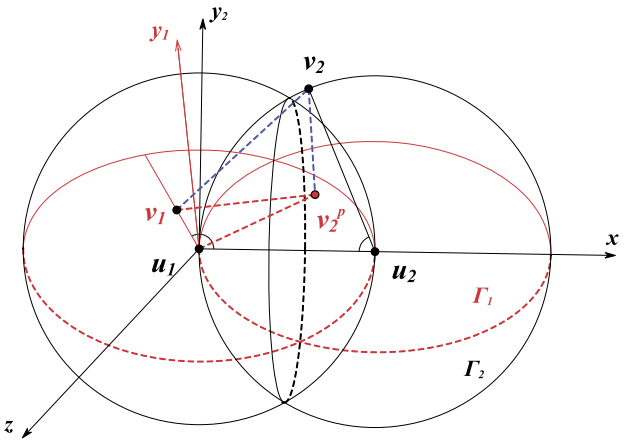

Fig. 13. Rectangular coordinate systems.

$$\begin{cases} \mu^2 = d^2(v_1, v_2) - d^2(v_2, v_2^p) = 1 - (\sin\theta_2 \sin\delta)^2 \\ \rho^2 = d^2(v_2, u_1) - d^2(v_2, v_2^p) = \left(2\sin\frac{\theta_2}{2}\right)^2 - (\sin\theta_2 \sin\delta)^2 \end{cases} \tag{8}$$

Note that both μ and ρ have nothing to do with r_1.

Using knowledge of analytical geometry, we have

$$\begin{aligned} &(r_1\cos\theta_1 - 1 + \cos\theta_2)^2 + (r_1\sin\theta_1 - \sin\theta_2\cos\delta)^2 = \mu^2 \\ \Rightarrow &\sin(\theta_1 + \phi) = \frac{r_1^2 - \mu^2 + \rho^2}{2r_1\rho} \text{ where } \tan\phi = \frac{1-\cos\theta_2}{\sin\theta_2\cos\delta}. \end{aligned} \tag{9}$$

Since $\tan\phi = \dfrac{1-\cos\theta_2}{\sin\theta_2\cos\delta} = \dfrac{\tan(\theta_2/2)}{\cos\delta} \geq \tan\dfrac{\theta_2}{2}$, then $\phi \geq \theta_2/2$. Besides, $\theta_1, \theta_2 \in [\pi/3, 2\pi/3]$. We have $\phi \in [\pi/6, \pi/3]$. Therefore, $\theta_1 + \phi \geq \pi/2$. Consequently,

$$\theta_1 = \pi - \phi - \arcsin\left(\frac{r_1^2 + \rho^2 - \mu^2}{2r_1\rho}\right).$$

Now, the value of $\left|P_1'M_1\right|$ is a function of r_1, θ_2 and δ. We denote it as $\alpha(r_1, \theta_2, \delta)$ and

$$\alpha(r_1, \theta_2, \delta) = \pi - \phi - \arcsin\left(\frac{r_1^2 + \rho^2 - \mu^2}{2r_1\rho}\right) + \arccos\frac{r_1}{2} - \frac{2\pi}{3}.$$

Considering μ, ρ, ϕ contribute nothing to $\partial\alpha(r_1, \theta_2, \delta)/\partial r_1$, we have

$$\frac{\partial\alpha(r_1, \theta_1, \delta)}{\partial r_1} = \frac{\rho^2 - \mu^2 - r_1^2}{2r_1^2\rho} \frac{1}{\sqrt{1 - \left(\dfrac{r_1^2 + \rho^2 - \mu^2}{2r_1\rho}\right)^2}} - \frac{1}{2}\frac{1}{\sqrt{1 - \left(\dfrac{r_1}{2}\right)^2}}.$$

Next, we will discuss two situations to analyze the monotonicity of $\partial\alpha(r_1, \theta_2, \delta)/\partial r_1$ with r_1.

Case 1: When $r_1^2 \geq \rho^2 - \mu^2$, it is easy to see that $\partial\alpha(r_1)/\partial r_1 \leq 0$ which means the value of $\alpha(r_1, \theta_2, \delta)$ decreases when r_1 increases.

Case 2: In this case, $r_1^2 < \rho^2 - c^2$. Next we will explore the increasing interval of r_1 for function $\alpha(r_1, \theta_2, \delta)$ when θ_2 and δ are fixed. If $\partial\alpha(r_1)/\partial r_1 > 0$, we have

$$\frac{\partial\alpha(r_1, \theta_2, \delta)}{\partial r_1} > 0 \Leftrightarrow \frac{1}{2r_1^2\rho}\sqrt{\frac{(\rho^2 - \mu^2 - r_1^2)^2}{1 - \left(\dfrac{r_1^2 + \rho^2 - \mu^2}{2r_1\rho}\right)^2}} - \frac{1}{2r_1^2\rho}\sqrt{\frac{(r_1^2\rho)^2}{1 - \left(\dfrac{r_1}{2}\right)^2}} > 0$$

$$\Leftrightarrow \left(\frac{\rho^2-\mu^2-r_1^2}{r_1^2\rho}\right)^2 > \frac{1-\left(\frac{r_1^2+\rho^2-\mu^2}{2r_1\rho}\right)^2}{1-\left(\frac{r_1}{2}\right)^2}$$

$$\Leftrightarrow \rho^2-\mu^2-r_1^2 > \mu r_1^2.$$

Therefore, $\alpha(r_1,\theta_1,\delta)$ is a monotone increasing function with r_1 when $r_1^2 < \frac{\rho^2-\mu^2}{1+\mu}$.

In conclusion, when $r_1^2 < \frac{\rho^2-\mu^2}{1+\mu}$, $\alpha(r_1,\theta_1,\delta)$ increases with r_1 increasing; when $r_1^2 > \frac{\rho^2-\mu^2}{1+\mu}$, $\alpha(r_1,\theta_1,\delta)$ decreases with r_1 increasing. Assuming $r_1 \in [r_1^{min}, 1]$, where r_1^{min} denotes the minimum r_1, the value of $\alpha(r_1,\theta_1,\delta)$ can be minimized only when $r_1 = r_1^{min}$ or $r_1 = 1$. Hence, Lemma 10 holds. □

For instance $(\delta, r_1, 1, \theta_1, \theta_2)$ with $d(v_1,v_2)=1$, β and δ are specified. Easy to see that smaller α results in smaller $d(P_1', P_2')$. Therefore, if $d(P_1', P_2') \geq 1$ for both the situations where $r_1 = r_1^{min}$ and $r_1 = 1$, we can declare that $d(P_1', P_2') \geq 1$ for all cases, according to Lemma 10. Therefore, what we need to do next is to verify $d(P_1', P_2') \geq 1$ for these two situations.

Case 1: **(r_1 is minimal):** For this case, we first need to figure out the minimal value of r_1 when θ_2 and δ are fixed. Considering v_1 locates in $B_1 \backslash B_2$, it is obvious that, when v_1 locates on the intersection of $disk(u_2)$ on plane Γ_1 with the unit ball whose center locates on v_2, r_1 reaches minimal. In this state, we use θ_1^{min} to denote the current θ_1. Then, $r_1^{min} = 2\cos\theta_1^{min}$. According to Equation (8) and Equation (9), we have

$$\begin{aligned}\mu^2 &= 1-(\sin\delta\sin\theta_2)^2 \\ &= \left[(1-\cos\theta_2) - r_1^{min}\cos\theta_1^{min}\right]^2 + \left[\sin\theta_2\cos\delta - r_1\sin\theta_1^{min}\right]^2.\end{aligned}$$

Finally, we have

$$\begin{cases} 2\sin 2\theta_1^{min}\sin\theta_2\cos\delta - 2\cos 2\theta_1^{min}\cos\theta_2 = 1 \\ r_1^{min} = 2\cos\theta_1^{min} \end{cases} \tag{10}$$

From Equation (10), when θ_2 and δ are given, we can figure out r_1^{min} and θ_1^{min}. Then, we can figure out the value of α and β. Furthermore, we can figure out the value of x, y and z in inequality (5). In order to prove $d(P_1', P_2') \geq 1$ in this case, we need to verify

$$\begin{aligned}\frac{x}{y} \leq \frac{1-z}{1+z} &\Leftrightarrow \frac{\cos(\theta_1^{min}-\frac{\pi}{6}+\frac{\theta_2}{2})}{\cos(\theta_1^{min}-\frac{\pi}{6}-\frac{\theta_2}{2})} = \frac{1-\tan(\theta_1^{min}-\frac{\pi}{6})\tan\frac{\theta_2}{2}}{1+\tan(\theta_1^{min}-\frac{\pi}{6})\tan\frac{\theta_2}{2}} \leq \frac{1-z}{1+z} \\ &\Leftrightarrow \tan(\theta_1^{min}-\frac{\pi}{6})\tan\frac{\theta_2}{2} \geq \cos\delta.\end{aligned} \tag{11}$$

Furthermore, for any fixed α and β, δ has a minimal value to satisfy $d(P_1', P_2') \geq 1$. Among those minimal values of δ, the maximal one is $\arccos\frac{1}{3}$ when $d(P_1', P_2') = 1$ and $\alpha = \beta = 0$. That is to say, once $\delta \geq \arccos\frac{1}{3}$, $d(P_1', P_2')$ will always be equal or larger than 1. Hence, in general case, we only need to consider the situation where $\delta \leq \arccos\frac{1}{3}$. According to Lemma 9, we can get the maximal value of β we need to consider. Therefore, the ranges of θ_2 and δ we need to consider are

$$\begin{cases} \delta \in \left[0,\ \arccos\frac{1}{3}\right] \\ \theta_2 \in \left[\frac{\pi}{3},\ 2\arctan\left(\frac{1-2\tan^2(\delta/2)}{\sqrt{3}}\right)+\frac{\pi}{3}\right]. \end{cases} \tag{12}$$

By numerical method, we can verify inequality (11) under conditions (12).

Case 2: **(r_1 is maximal):** It is easy to figure out that the minimal value of r_1 is 1 when v_1 locates on $Sur(B_1)$. In this case, P_1' and v_1 are the same. $d(P_1', P_2') = d(v_1,v_2) = 1$ which meets the requirement in Theorem 5.

In conclusion, according to the analysis in Sections 3.1 and 3.2, Theorem 5 always follows. Therefore, we can use our new projection rule to fix the incorrectness in [1].

Algorithm 1 C-CDS-UBG($G(V, E)$).

Set $M = \Phi$, $B = \Phi$, $V' = V$.
Pick a root $r \in V'$ that r has the biggest degree in V'.
Set $M = \{r\}$, $B = N(r)$, $V' = V' \backslash N[r]$.
while $V' \neq \Phi$ **do**
  Pick a node $u \in N(B)$ such that $|N(u) \cap V'|$ is maximized.
  Set $M = M \cup \{u\}$, $B = B \cup (M \cap V')$, and $V' = V' \backslash N(u)$.
end while
Set $C = \{r\}$ and $M' = M = \{r\}$.
while $M' \neq \Phi$ **do**
  Pick a node $v \in N(C)$ such that $|M_{v,C}| = max\{|M_{u,c}| u \in N(C)\}$.
  Set $C = C \cup \{v\} \cup M_{v,C}$ and $M' = M' \backslash M_{v,C}$.
end while
Return C.

Algorithm 2 CUTLEAF(u).

Set $P = Dom(u)$.
while $P \neq \Phi$ **do**
  Pick a node $x \in P$.
  if x has not been visited **then**
    CUTLEAF(x).
  end if
  Set $P = P \backslash \{x\}$.
end while
if ($|Dom(v)| \geq 2$ for all $v \in N(u)$ in graph G) and $|Dom(u)| = 1$ **then**
  $C = C \backslash \{u\}$.
end if
Return C.

4. MCDS construction improvement

So far, we have analyzed the approximation ratio of the MIS in UBG. In this section, we will introduce two prune methods to improve Kim's CDS construction algorithm. The following are some notations used in this section:

1) For node u, $N(u) = \{v | v \in V(G) \backslash u$ and $d(u, v) \leq 1\}$, $N[u] = N(u) \cup \{x\}$.
2) For node set C, $N(C) = (\cup_{v \in C} N(v)) \backslash C$.
3) For u and C, $M_{u,C} = \{v | d(u, v) \leq 1,\ v$ is a MIS node and $v \notin C\}$.
4) For u, $Dom(u) = \{v | d(u, v) \leq 1$ and v is a CDS node$\}$.

4.1. Algorithm for computing CDS

The algorithm introduced by Kim is formally described in Algorithm 1, which has two steps. It firstly generates an MIS M such that every node in M has at least one 2-hop neighbor and no 1-hop neighbors. We can use Butenko and Ursulenko's algorithm to compute such MIS. The second step is to connect this MIS. Kim used a greedy strategy, which starts with the original node and repeats round by round. In each round, it picks a node v adjacent to the connected component C computed in the previous rounds that makes $|M_{v,C}|$ maximal, and add it to C, it terminates when all the points in MIS are connected.

4.2. Improve the generated CDS

In this 2-step algorithm, there is some redundancy in the given CDS C. Firstly, through the computing of MIS, some nodes which have only one neighbor may be added to the MIS in order to maintain the properties of MIS. But when the connectors are added, those points would be useless for the whole CDS, and it is better to adjust it to non-CDS nodes. Also, the redundancy may occur in the inner side of the CDS due to the increased density of CDS nodes. Since the redundancy occurs after the algorithm terminates, we can add two more steps afterward to reduce CDS size with the help of prune techniques.

Notice that once we remove a CDS node, the remaining CDS must maintain all its original properties. Thus for a CDS node $u \in G$, it could be removed iff:

1. Every point that u dominates must have at least one alternative dominator.
2. $G(C \backslash \{u\})$ is connected.

Correspondingly, we design two prune methods to reduce CDS size. The first method is to reduce some leaf nodes instantly. We use postorder traversal to traverse the CDS tree and reduce redundant points in it, as shown in Algorithm 2.

Algorithm 3 CUTINSIDE($G(V, E), C$).

1: Let G' be the subgraph generated by C, compute all the congestion nodes $C' \in C$.
2: Pick up a node $u \in V$ s.t. $u \notin C'$ and ($|Dom(v)| \geq 2$ for all $v \in N(u)$ in G).
3: $C = C \backslash \{u\}$. Return.

Algorithm 4 R-C-CDS-UBG($G(V, E)$).

1: $P =$ C-CDS-UBG($G(V, E)$), pick a root $r \in V'$ that r has the biggest degree in V'.
2: Run CUTLEAF(r).
3: Run CUTINSIDE($G(V, E), P$) for several(30) times.
4: Return P.

Lemma 11. *For any CDS C, after Algorithm 2 is executed, C is also a CDS.*

Proof. Let C' be the CDS after Algorithm 2 is executed. If $C' = C$, then Lemma 11 holds. Otherwise, let C_0 be the initial CDS, C_i be the CDS after the i-th reduction and u_i be the node reduced in this iteration. We show that if C_i is a CDS, then C_{i+1} is a CDS, for $i \geq 0$. According to Line 9, all $N(u_{i+1})$ has at least 2 dominators. Also, $|Dom(u_{i+1}) = 1|$ ensures that only one CDS node is adjacent to u_{i+1}. So $C_{i+1} = C_i \backslash \{u_{i+1}\}$ is also connected. Hence, C_{i+1} is a CDS. Since C_0 is a CDS, recursively after Algorithm 2 is executed, C' is also a CDS. □

Lemma 12. *For any CDS C, after Algorithm 3 is executed, C is also a CDS.*

Proof. Similar to Lemma 2, Line 2 ensures that all $N(u)$ has at least 2 dominators. Moreover, u is not a congestion node ensures that $C \backslash \{u\}$ is connected. □

With two algorithms above, Algorithm 4 is an improvement for computing CDS.

Theorem 13. *The time and space complexity of Algorithm 4 R-C-CDS-UBG is $O(n^2)$, where n is the number of nodes in a given input UBG.*

Proof. Since it is necessary to store the graph, the space complexity of Algorithm 4 is $O(n^2)$. Then we show that the time complexity is $O(n^2)$.

Firstly, the input time complexity for Algorithm 4 is $O(n)$. For the first step of Algorithm 1 (Lines 1–7), each round of the while loop add one point to the MIS, so the while loop ends in $O(n)$ rounds. In each round, a node x should be picked. Since we can store and update it instantly, the time complexity of node selection is $O(n)$ each round. Thus the time complexity of the whole loop is $O(n^2)$.

For the second step of Algorithm 1 (Lines 8–13), since each round of the while loop joined at least one MIS point to the CDS, and the MIS has $O(n)$ nodes, the loop ends in $O(n)$ rounds. During each round, we use an array to store $|M_{v,C}|$, and the maintenance time complexity is $O(n)$, since only points in $N(N(v))$ would change its $|M_{v,C}|$. Also, the time complexity to select a v is $O(n)$ each round. Hence, the time complexity of Algorithm 1 is $O(n^2)$.

For Algorithm 2, we can store $|Dom(u)|$ for each $u \in G$. Once a CDS node v is reduced, only $Dom(N(v))$ nodes need to change, so the maintenance complexity is $O(n)$. Next, each edge in G will be visited for a constant times, so the overall time complexity is $O(n^2)$. For Algorithm 3, we can use Tarjan's strongly connected components algorithm for computing congestion set C', whose time complexity is $O(n^2)$. Hence, the time complexity of Algorithm 3 is $O(n^2)$.

For Algorithm 4, it runs Algorithm 1 once, Algorithm 2 once, and Algorithm 3 for a constant time, each with time $O(n^2)$. Therefore, the time complexity of Algorithm 4 is $O(n^2)$. □

5. Simulation results

In this section, we compare Algorithm 4 with Kim's Algorithm 1 to solve MCDS in UBGs. For the simulations, we deploy wireless nodes in a $20 \times 20 \times 20$ three-dimensional virtual space. We also ensure that the graph induced by all nodes is connected. The number of nodes varies from 100 to 1000 by increasing 100. We use 1 as the maximum transmission range of the nodes. Through the random graph generation process, we control the lower bound of distance between two nodes at 0.25, 0.5, 0.75. Thus, we can have graphs with different node density. In Fig. 14, we use R-C-CDS-UBG to identify our algorithm, and C-CDS-UBG to identify Kim's.

Fig. 14 shows the comparison of the performance between two algorithms when the lower bound of distance between two points is 0.25, 0.5, and 0.75 respectively. Through the figure, we can see that whatever the graph is, our algorithm can give a better answer than Kim's averagely. The ratio between our answer and Kim's is nearly 0.78. Also, through the comparison, we can figure out that in most situations, our improvement is steady.

Fig. 15 shows a sample of UBG which has 500 points. The first picture is the result by Kim's algorithm with 208 CDS points, while the second is the result by prune algorithm with 155 CDS points. In this example our algorithm reduces CDS size by 25%, and it can be found in the graph where lots of the boundary nodes are dropped to make the CDS much smaller.

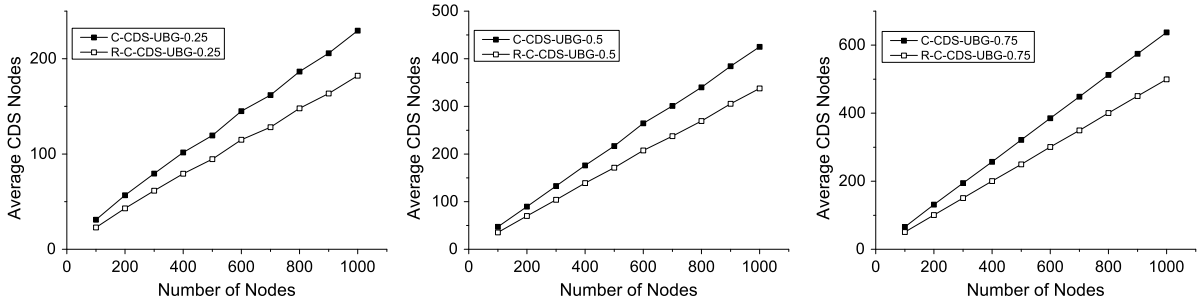

Fig. 14. Comparison with different parameter settings.

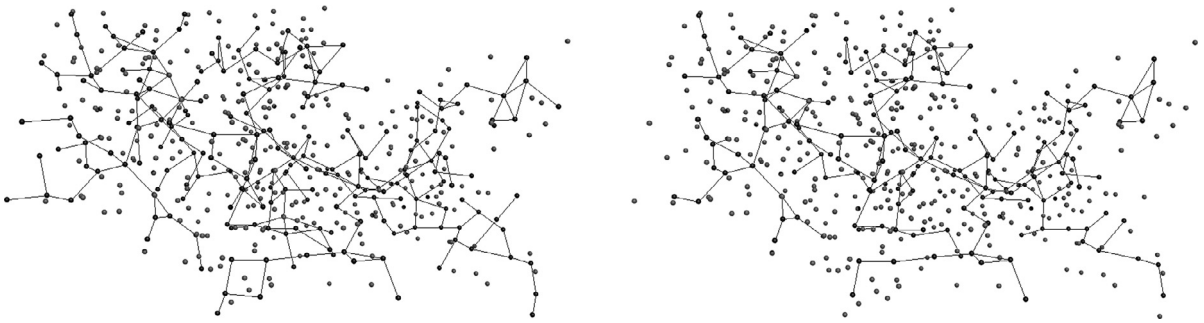

(a) CDS by Kim's Algorithm 1. |CDS|=208

(b) CDS by Prune Algorithm 4. |CDS| = 155

Fig. 15. An example solution with $n = 500$ points.

6. Conclusion

In this paper, we first pointed out the problem in Kim's method [1]. Then, we proposed a new projection method for solving the *two-ball problem*. With this new projection method, we successfully improved the ratio of $mis(G)/mcds(G)$ in UBG into 10.917. Moreover, we also optimized the algorithm for minimum connected dominating set selection in [1] with prune process and validate the efficiency of our design by numerical experiments.

Acknowledgement

This work has been supported in part by the National Natural Science Foundation of China (Grant number 61202024, 61472252, 61133006, 61422208), China 973 project (2014CB340303), Shanghai Educational Development Foundation (Chenguang Grant No. 12CG09), Science and Technology Commission of Shanghai Municipality (Pujiang Grant No. 13PJ1403900), the Natural Science Foundation of Shanghai (Grant No. 12ZR1445000), and in part by Jiangsu Future Network Research Project No. BY2013095-1-10 and CCF-Tencent Open Fund. The opinions, findings, conclusions, and recommendations expressed in this paper are those of the authors and do not necessarily reflect the views of the funding agencies or the government. We also would like to thank Mr. Fengwei Gao and Ms. Ling Ding for their contributions on the early versions of this paper.

References

[1] D. Kim, Z. Zhang, X. Li, W. Wang, W. Wu, D.-Z. Du, A better approximation algorithm for computing connected dominating sets in unit ball graphs, IEEE Trans. Mob. Comput. 9 (8) (2010) 1108–1118.
[2] J. Liu, H. Nishiyama, N. Kato, J.-f. Ma, X. Jiang, Throughput-delay tradeoff in mobile ad hoc networks with correlated mobility, in: IEEE International Conference on Computer Communications (INFOCOM), 2014, pp. 2768–2776.
[3] M.B. Younes, A. Boukerche, A traffic balanced mechanism for path recommendations in vehicular ad-hoc networks, in: IEEE Global Communications Conference (GLOBECOM), 2014, pp. 45–50.
[4] M. Benter, H. Frey, et al., Reactive planar spanner construction in wireless ad hoc and sensor networks, in: IEEE International Conference on Computer Communications (INFOCOM), 2013, pp. 2193–2201.
[5] B. Tang, B. Ye, S. Lu, S. Guo, I. Stojmenovic, Latency-optimized broadcast in mobile ad hoc networks without node coordination, in: ACM International Symposium on Mobile Ad Hoc Networking and Computing (MOBIHOC), 2014, pp. 317–326.
[6] Y. Hong, D. Bradley, D. Kim, D. Li, A.O. Tokuta, Z. Ding, Construction of higher spectral efficiency virtual backbone in wireless networks, Ad Hoc Netw. 25 (2015) 228–236.
[7] Y. Dai, J. Wu, C. Xin, Efficient virtual backbone construction without a common control channel in cognitive radio networks, IEEE Trans. Parallel Distrib. Syst. 25 (12) (2014) 3156–3166.
[8] M.A. Togou, A. Hafid, P.K. Sahu, A stable minimum velocity cds-based virtual backbone for vanet in city environment, in: IEEE Conference on Local Computer Networks (LCN), 2014, pp. 510–513.

[9] J.S. He, S. Ji, Y. Pan, Y. Li, Greedy construction of load-balanced virtual backbones in wireless sensor networks, Wirel. Commun. Mob. Comput. 14 (7) (2014) 673–688.
[10] M. Kouider, P.D. Vestergaard, et al., Generalized connected domination in graphs, Theoret. Comput. Sci. 8 (1) (2006) 57–64.
[11] S. Gaspers, M. Liedloff, et al., A branch-and-reduce algorithm for finding a minimum independent dominating set, Theoret. Comput. Sci. 14 (1) (2012) 29–42.
[12] A. Gonzalez, Ó. Lázaro, S. Vaz, Deploying and experimenting wireless ad hoc networks in mountainous regions for broadband multimedia service access, in: International ICST Mobile Multimedia Communications Conference (MOBIMEDIA), 2009, pp. 21–27.
[13] D.D. Tan, D.-S. Kim, Cooperative transmission scheme for multi–hop underwater acoustic sensor networks, Int. J. Commun. Netw. Distrib. Syst. 14 (1) (2015) 1–18.
[14] X.-h. Wang, P.-f. Li, Improved data association method in binocular vision-slam, in: IEEE Intelligent Computation Technology and Automation (ICICTA), 2010, pp. 502–505.
[15] D. Yang, An immunity-based ant colony optimization topology control algorithm for 3d wireless sensor networks, Sens. Transducers J. 150 (3) (2013) 125–129.
[16] P.-J. Wan, K.M. Alzoubi, O. Frieder, Distributed construction of connected dominating set in wireless ad hoc networks, in: IEEE International Conference on Computer Communications (INFOCOM), 2002, pp. 1597–1604.
[17] W. Wu, H. Du, X. Jia, Y. Li, S.C.-H. Huang, Minimum connected dominating sets and maximal independent sets in unit disk graphs, Theoret. Comput. Sci. 352 (1) (2006) 1–7.
[18] X. Gao, Y. Wang, X. Li, W. Wu, Analysis on theoretical bounds for approximating dominating set problems, Discrete Math. Algorithms Appl. 1 (1) (2009) 71–84.
[19] M. Li, P.-J. Wan, F. Yao, Tighter approximation bounds for minimum cds in unit disk graphs, Algorithmica 61 (4) (2011) 1000–1021.
[20] Y.L. Du, H.W. Du, A new bound on maximum independent set and minimum connected dominating set in unit disk graphs, J. Comb. Optim. (2013) 1–7.
[21] C. Zong, Sphere Packings, vol. 3, Springer, 1999.
[22] J.C. Hansen, E. Schmutz, Comparison of two cds algorithms on random unit ball graphs, in: Algorithm Engineering and Experiments & Analytic Algorithmics and Combinatorics (ALENEX/ANALCO), 2005, pp. 206–211.
[23] S. Butenko, S. Kahruman-Anderoglu, O. Ursulenko, On minimum connected dominating set problem in unit-ball graphs, Optim. Lett. 5 (2011) 195–205.
[24] X. Zhong, J. Wang, N. Hu, Connected dominating set in 3-dimensional space for ad hoc network, in: IEEE Wireless Communications and Networking Conference (WCNC), 2007, pp. 3609–3612.
[25] F. Zou, X. Li, D. Kim, W. Wu, Construction of minimum connected dominating set in 3-dimensional wireless network, in: International Conference on Wireless Algorithms, Systems, and Applications (WASA), 2008, pp. 134–140.
[26] D.-Z. Du, P.-J. Wan, Connected Dominating Set: Theory and Applications, vol. 77, Springer, 2012.